Research article

RHBDF1 modulates cisplatin sensitivity of small cell lung cancer through YAP1/Smad2 signaling pathway

Lei Wang [a], Lishuang Qi [b], Xiaoyi Huang [c,g], Xiao Feng [d], Junqing Gan [e], Juxuan Zhang [b], Yuhui Xi [f], Shuai Zhang [a], Qingwei Meng [a,*]

[a] Department of Medical Oncology, Harbin Medical University Cancer Hospital, Harbin, Heilongjiang, 150081, China
[b] College of Bioinformatics Science and Technology, Harbin Medical University, Harbin, Heilongjiang, 150081, China
[c] Biotherapy Center, Harbin Medical University Cancer Hospital, Harbin, Heilongjiang, 150081, China
[d] Department of Oncology, Jinan Central Hospital Affiliated to Shandong University, Jinan, Shandong, 250013, China
[e] Department of Radiation Oncology, North China University of Science and Technology Affiliated Hospital, Tangshan, 063000, China
[f] Department of Pathophysiology, Harbin Medical University, Harbin, Heilongjiang, 150081, China
[g] NHC Key Laboratory of Cell Transplantation, Harbin Medical University, Harbin, Heilongjiang, 150081, China

A R T I C L E   I N F O

A B S T R A C T

Small cell lung cancer (SCLC) is a fatal tumor type that is prone to drug resistance. In our previous study, we showed that human rhomboid-5 homolog-1 (RHBDF1) was differentially expressed in 5 intrinsic cisplatin-resistant SCLC tissues compared with 5 intrinsic cisplatin-sensitive SCLC tissues by RNA sequencing, which intrigued us. We performed gain- and loss-of-function experiments to investigate RHBDF1 function, bioinformatics analysis, qRT-PCR, western blotting, and immuno-precipitation to elucidate the molecular mechanisms as well as detect RHBDF1 expression in SCLC by immunohistochemistry. We found that RHBDF1 knockdown promoted cell proliferation and cisplatin chemoresistance and inhibited apoptosis in *vitro* and in *vivo*. These effects could be reversed by overexpressing RHBDF1 in *vitro*. Mechanistically, RHBDF1 interacted with YAP1, which increased the phosphorylation of Smad2 and transported Smad2 to the nucleus. Among clinical specimens, the RHBDF1 was a low expression in SCLC and was associated with clinico-pathological features and prognosis. We are the first to reveal that RHBDF1 inhibited cell pro-liferation and promoted cisplatin sensitivity in SCLC and elucidate a novel mechanism through RHBDF1/YAP1/Smad2 signaling pathway which played a crucial role in cisplatin chemo-sensitivity. Targeting this pathway can be a promising therapeutic strategy for chemotherapy resistance in SCLC.

1. Introduction

Small cell lung cancer (SCLC), is one of the predominant pathological types of lung cancer, which accounts for 13–15 % of all lung cancer cases [1]. So far, chemotherapy is still validated as a standard treatment for SCLC [2], and immunotherapy has improved the prognosis for patients to a certain extent [3,4]. No specific and effective treatment has been developed to date. Therefore, further elucidating the molecular mechanisms underlying SCLC chemotherapy resistance is crucial.

Based on the present treatment strategies, we detected that human rhomboid-5 homolog-1 (RHBDF1) was differentially expressed

---

Abbreviations

SCLC	Small cell lung cancer
RHBDF1	Human rhomboid-5 homolog-1
GPCR	G protein-coupled receptor
EGFR	Epidermal growth factor receptor
EMT	Epithelial-to-mesenchymal transition
MDR	Multidrug resistance
DEGs	Differentially expressed genes
GEO	Gene expression omnibus
TNM	Tumor node-metastasis
HBE	Human bronchial epithelial
qRT-PCR	quantitative reverse transcriptase polymerase chain reaction
CCK-8	Cell Counting Kit-8
SD	Standard deviation
GO	Gene ontology
BP	Biological processes
CC	Cellular components
MF	Molecular function
KEGG	Kyoto Encyclopedia of Genes and Genomes
KM	Kaplan–Meier
OS	Overall survival
DFS	Disease-free survival

in SCLC tissues of 5 intrinsic cisplatin-resistance and 5 intrinsic cisplatin-sensitivity by RNA sequencing [5,6]. RHBDF1 is a multi-transmembrane protein mainly located in the Golgi membrane and endoplasmic reticulum membrane [7,8]. RHBDF1 is a molecular switch that suppresses HIF1α degradation by interacting with the receptor of activated protein-C kinase-1 in breast cancer [9]. RHBDF1 regulates epithelial-to-mesenchymal transition (EMT) and proliferation through the Wnt/β-catenin pathway in colorectal cancer [10,11]. RHBDF1 knockdown inhibited cell proliferation, regulated cell cycle, and induced apoptosis by downregulating the expression of β-catenin, Myc, p-EGFR, and TGFBR2 and upregulating the expression of FAS in HeLa cells. RHBDF1 overexpression was associated with clinical features in cervical cancer [4]. However, the specific role and underlying molecular mechanisms of RHBDF1 in SCLC are yet to be identified.

Based on the expression of transcriptional factors, namely ASCL1, NEUROD1, YAP1, and POU2F3, a study has suggested that SCLC can be classified into four distinct molecular subtypes, namely SCLC-A, SCLC-N, SCLC-Y, and SCLC-P, with distinct biology and therapeutic responses [12]. Many studies have shown that YAP1 plays a role in multidrug resistance (MDR). Song et al. suggested that YAP1 can induce MDR via CD74 inhibiting the apoptosis of SCLC [13]. A further study showed that WW domain binding protein 5 can regulate MDR by decreasing YAP1 phosphorylation levels at Serine 127 and inducing nuclear accumulation of YAP1 [14]. Interestingly, many studies suggested that there is a crosstalk between Hippo and TGF-β signaling pathways. A previous study showed that TGF-β can induce the complex formation of YAP/TAZ-Smad2/3 in HaCaT cells, thereby coordinating cellular processes [15]. A study showed that Resveratrol inhibited the EMT of gastric cancer by downregulating the Hippo/YAP1 signaling pathway [6,7]. Notably, RASSF1A degradation facilitated YAP1 and Smad2 interaction and subsequent nuclear translocation of Smad2 [16]. However, the roles of YAP1 and Smad2 in the chemoresistance of SCLC are yet to be completely understood.

In our study, based on bioinformatic analysis, we found that RHBDF1 was downregulated in SCLC and associated with overall survival (OS). Further studies showed that RHBDF1 suppressed proliferation and mediated cisplatin chemosensitivity by promoting apoptosis in *vitro* and in *vivo*. Subsequent studies showed that RHBDF1 interacts with YAP1 and contributes to the nuclear translocation of Smad2, thereby activating the Smad2 signaling pathway. Moreover, RHBDF1 expression has been determined in tissues obtained from 123 patients with SCLC and 71 adjacent lung tissue samples and associated with clinicopathological features. Therefore, in this study, we elucidated a new mechanism underlying the cisplatin chemoresistance in SCLC and provided a rationale for targeting RHBDF1 as a novel strategy to inhibit chemoresistance in SCLC.

2. Materials and methods

2.1. Data collection and bioinformatics analysis

GSE149507 and GSE40275 gene chip datasets obtained from Gene expression omnibus (GEO, https://www.ncbi.nlm.nih.gov/gds/) were employed to analyze the gene expression profiles, while the GSE60052 RNA sequencing dataset was used to verify the gene expression and for the subsequent analyses of clinical prognosis. NetworkAnalyst (https://www.networkanalyst.ca/) [4,13,17] was used to perform cluster analysis and *t*-SNE drawing for the GSE149507 dataset. Functional enrichment analysis was conducted using the R 4.0.2 software. We employed the STRING database (https://cn.string-db.org/) to predict the protein–protein interactions [18].

2.2. Clinical specimens

The clinical specimens were collected between March 2014 and May 2020 and included 123 cases of surgical resection SCLC and 71 cases of adjacent lung tissues. Among these, 78 patients (63.41 %) were men and 45 (36.59 %) were women. The age of the patients ranged from 34 to 75 years (median age: 60 years). Tumor node-metastasis (TNM) classification was performed with reference to the 8th edition of the International Union Against Cancer System. The patients were followed until January 2022 or death or until the loss to follow-up; the median follow-up period was 53.7 months.

2.3. Cell lines

The human SCLC cell lines H446, H82, SHP77, H2227, and H1092 were purchased from the Cell Bank of the Chinese Academy of Sciences (Shanghai, China), and human bronchial epithelial (HBE) cells were provided by Heilongjiang Cancer Institute (Harbin, China). All cells were authenticated by short-tandem repeat (STR) analysis before being used for the experiments. The cells were maintained in the RPMI 1640 medium (HyClone, USA) supplemented with 10 % fetal bovine serum (Pan-Biotech, Germany) and 100 mg/mL penicillin–streptomycin (Hyclone, USA). All cells were kept at 37 °C in a 5 % carbon dioxide atmosphere.

2.4. Construction of stable cell lines

To stably overexpress RHBDF1 or YAP1, H446 cells were transfected with pLVX-Puro-RHBDF1-Flag or pLVX-Puro empty vector (Ousai Biotech, Shanghai, China) and pCMV-zsG-Puro-YAP1 or pCMV-zsG-Puro vector (Genechem Biotech, Shanghai, China) using jetPRIME® (Polyplus-transfection® SA, Strasbourg, France). Briefly, 2×10^5 cells were seeded into a 6-well plate with 2 mL of the culture medium per well 24 h before transfection. JetPRIME® reagent was applied to transfect the above-mentioned vectors when the cell confluence reached 60–80 %. After replacing the medium 4 h after transfection, the cells were continuously cultured for 24–48 h before screening with 0.5 μg/mL of puromycin. The surviving cells were cultured for further identification and experiments. According to the manufacturer's protocol, H2227 cells were transfected with hU6-MCS-CBh-gcGFP-IRES-puro-RHBDF1 or hU6-MCS-CBh-gcGFP-IRES-puro empty vector, these lentiviral shRNA were sourced from Genechem Biotechnology (Shanghai, China).

2.5. Real-time PCR

Total RNA from the cells was extracted with TRIzol reagent (Invitrogen, Carlsbad, USA) in accordance with the manufacturer's protocol. RNA was reverse transcribed into cDNA using the FastKing gDNA Dispelling RT Supermix Kits (TIANGEN Biotech, Beijing, China). The FastStart Universal SYBR Green Master Rox (Roche, Switzerland) and StepOnePlus Real-time PCR System (Applied Biosystems, USA) were used for qRT-PCR. GAPDH was used as the internal reference. The primers used in this study are listed in Table S1.

2.6. Western blotting

Western blotting was performed as described elsewhere [19,20]. Details for all the antibodies used are provided in Table S2. Cytosolic and nuclear protein extractions were performed using the Cytoplasmic and Nuclear Extraction Kit (Beyotime, Shanghai, China) in accordance with the manufacturer's instructions.

2.7. Cell proliferation assays

For this assay, 5×10^3 cells/well were seeded into a 96-well plate and examined on 0–72h by using the Cell Counting Kit-8 (CCK-8) kit (MCE, China) at 450 nm absorbance to observe cell viability. However, 8×10^3 cells/well were seeded into a 96-well plate and examined on 24h by using the CCK-8 kit (MCE, China) at 450 nm absorbance to detect the cell sensitivity to cisplatin. In addition, the YF®594 Click-iT EdU Imaging Kit (Bioscience, Shanghai, China) was used to detect cell proliferation and visualize the same by fluorescence microscopy as per the manufacturer's instructions.

2.8. Apoptosis analysis

The experimental cells were digested with EDTA-free trypsin and washed twice with PBS, after which 5 μL of Annexin V-APC and 5 μL 7-AAD (KeyGEN BioTECH, Nanjing, China) were sequentially added to the cell suspension and incubated for 15 min at room temperature in the dark. Flow cytometry was performed to determine cell apoptosis (Beckman CytoFLEX, USA).

2.9. Immunoprecipitation

The cell protein samples were collected as described in the Western blotting section for further analyses. Protein A/G magnetic beads (MCE, China) were prewashed thrice with 400 μL of the binding buffer and incubated with the indicated concentration of antibody for 1 h at room temperature on a rotating incubator, resulting in the formation of magnetic beads–antibodies complexes, in which 400 μL of the prepared protein samples were added and mixed with rotation at 4 °C overnight. The antigen–antibody magnetic

bead complex was washed 5 times with phosphate-buffered saline containing Tween detergent (PBST). After the addition of 60 µL of 1 × SDS–PAGE loading buffer, the lysate was boiled for 5 min to prepare for Western blotting.

2.10. Xenograft model

Five-week-old female BALB/c nude mice were purchased from Beijing Vital River Laboratory. A total of 5×10^6 H2227 cells were stably transfected with shNC or shRHB and subcutaneously injected into the left axilla of the experimental mice. For cisplatin treatment, 5 mg/kg cisplatin was injected thrice intraperitoneally every alternate day. SB431542 (Beyotime, Shanghai, China) was injected intraperitoneally (6 mg/kg, every alternate day for 7 times). The tumor size was calculated twice a week, and the tumor volume was calculated using the following formula: $0.5 \times$ lengths × width × width. The mice were sacrificed when the maximum tumor diameter
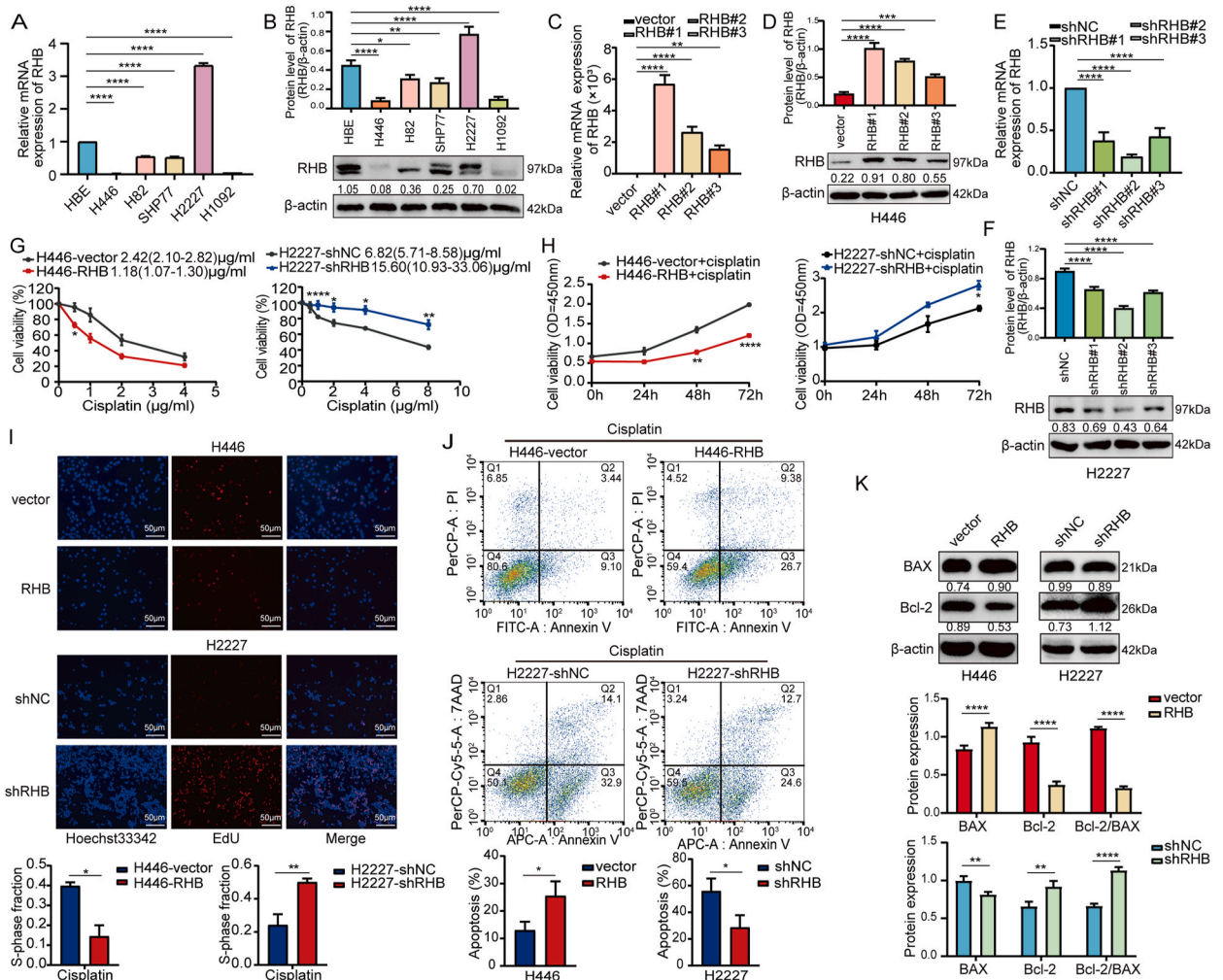
Fig. 1. RHBDF1 increased sensitivity of SCLC cells to cisplatin. The mRNA and protein levels of RHBDF1 were detected in HBE cells and SCLC cells by qRT-PCR (HBE was normalized to 1) (A) and western blotting (B). RHBDF1 overexpression in H446 cells were verified by qRT-PCR (C) and western blotting (D) after stably transfected with pLVX-Puro-RHBDF1-Flag recombinant vector or pLVX-Puro empty vector. The expression of RHBDF1 in H2227 cells were verified by qRT-PCR (shNC was normalized to 1) (E) and western blotting (F) after stably transfected with lentiviruses shRHBDF1 (shRHB#1, 2, 3) or empty vector. H446-RHB (left panel), H2227-shRHB (right panel) and corresponding control cells were treated with gradually increased concentration of cisplatin for 24 h, and cell viability was determined by a CCK-8 assay. The IC50 value of H446-vector was 2.42 (2.10–2.82) µg/mL, while the IC50 value of the H446-RHB was 1.18 (1.07–1.30) µg/mL. The IC50 value of H2227-shNC was 6.82 (5.71–8.58) µg/ mL, while the IC50 value of the H2227-shRHB was 15.60 (10.93–33.06) µg/mL (G). Cell proliferation was analyzed by a CCK-8 assay at 0, 24, 48, 72h (H) and an EdU incorporation assay at 72h (I) both in RHBDF1-overexpressing H446 cells and RHBDF1-knockdown H2227 cells with 0.5 µg/mL cisplatin for 24 h. The apoptotic rate was detected by flow cytometric analysis in H446-RHB cells and H2227-shRHB cells treated with 0.5 µg/mL cisplatin for 24 h (J). The protein levels of apoptosis markers were examined by western blotting in H446-RHB cells and H2227-shRHB cells with treatment of 0.5 µg/mL cisplatin for 24 h (K). β-actin was normalized to 1 in western blotting. N = 3 technical replicates, experiment was repeated at least 3 times. (*p < 0.05, **p < 0.01, ****p < 0.0001).

reached 1.5 cm or after 30 days of inoculation.

2.11. Immunohistochemistry

Immunohistochemistry was performed as described previously [19,20]. The immunostaining intensity was scored 0, negative staining; 1 +, weak staining; 2 +, moderate staining; 3 +, strong staining. The percentage of positive cells was assigned as follows: 0, 0 %; 1, ≤10 %; 2, 10–50 %; 3, >50 %. The final scores were calculated as the staining intensity multiplied by the staining percentage.

2.12. Statistical analysis

Statistical analysis was performed with SPSS 22.0 and GraphPad Prism 8. All data were presented as the mean ± standard deviation (SD). Student's *t*-test for two groups comparisons and one-way ANOVA was used for multi-groups comparisons, two-way ANOVA was used for multi-groups with two variables comparisons. All experiments were repeated at least three times, and $p < 0.05$ was considered to indicate statistical significance.

3. Results

3.1. RHBDF1 is downregulated in SCLC and correlated with clinical prognosis

Based on the differentially expressed genes (DEGs) that were identified by RNA sequencing in SCLC tissues, we investigated the following different datasets to determine the expression pattern of RHBDF1 in SCLC. GSE149507 dataset [21] showed that the tumor tissues and adjacent lung tissues were well clustered, and 1118 differential expression genes were screened (|logFC| >0.7, adjust p < 10^6, Figs. S1A–B). Among these genes, RHBDF1 was downregulated in SCLC compared with adjacent lung tissues (Figs. S1A and C). We then used GSE60052 [14,22] and GSE40275 datasets [23] to further investigate the expression of RHBDF1 in SCLC.As shown in Figs. S1D and E, the expression of RHBDF1 in SCLC was lower than that in normal lung tissues. Based on the GSE60052 dataset, KM analysis revealed that the group with higher RHBDF1 expression correlated with better OS when we ruled out 31 SCLC cases with incomplete clinical information (Fig. S1F, log-rank p = 0.0065). Using the complete clinical data of 77 SCLC cases sequenced by George, J et al. [24] to determine the relationship between RHBDF1 expression and OS. The results showed that high expression of RHBDF1 had a better OS, which is consistent with the results of the GSE60052 dataset (Fig. S1G, log-rank p = 0.022).

3.2. RHBDF1 suppressed cell proliferation and increased sensitivity of SCLC cells to cisplatin

RHBDF1 expression was evaluated in HBE cells and SCLC cell lines, in which RHBDF1 was significantly downregulated in almost all of the SCLC cell lines compared with normal lung epithelial cell by qRT-PCR (Fig. 1A) and western blotting (Fig. 1B). In addition, we found that the expression of RHBDF1 was highest in H2227 cells and lowest in H446 cells, so we chose these two typical cell lines for further study. After the overexpression and knockdown efficiencies were determined by western blotting and qRT-PCR (Fig. 1C–F), cell colony H446-RHB#1 and colony H2227-shRHB#2 were chosen for subsequent experiments. RHBDF1 overexpression significantly reduced the growth of H446-RHB cells, whereas RHBDF1 knockdown in H2227-shRHB cells accelerated cell growth by using CCK-8 and EdU assay (Figs. S2A–B). Furthermore, flow cytometry and western blotting assays were performed to determine cell apoptosis. The apoptosis rate was increased in H446-RHB cells, and the opposite results were confirmed in H2227-shRHB cells (Fig. S2C). Accordingly, western blotting results showed that the Bcl2/BAX ratio was reduced in H446-RHB cells and that was increased in H2227-shRHB cells (Fig. S2D). Overall, these results suggested that RHBDF1 negatively regulates cell proliferation by adjusting apoptosis *in vitro*.Fig. 1G showed that H446-RHB cells were more sensitive to cisplatin, whereas H2227-shRHB cells were less sensitive. We then performed a CCK-8 assay and an EdU assay to analyze cell viability at the dose of 0.5 μg/mL cisplatin for 24 h. As shown in Fig. 1H and I, RHBDF1 overexpression significantly decreased the cell viability and DNA incorporation rate of H446-RHB cells, whereas RHBDF1 depletion significantly increased the cell viability and DNA incorporation rate of H2227-shRHB cells when these cells were exposed to cisplatin treatment, which suggested that RHBDF1 regulated the cisplatin sensitivity in SCLC cells. Flow cytometry showed that RHBDF1 overexpression significantly increased the apoptosis of H446-RHB cells, whereas RHBDF1 knockdown decreased the apoptosis of H2227-shRHB cells with cisplatin for 24 h (Fig. 1J). Furthermore, western blotting showed that the Bcl2/BAX ratio was decreased in H446-RHB cells and increased in H2227-shRHB cells 24 h after cisplatin treatment at 0.5 μg/mL (Fig. 1K). Overall, our results suggested that RHBDF1 positively regulated cisplatin sensitivity by modulating apoptosis *in vitro*.

3.3. Functional enrichment analysis of RHBDF1

To further elucidate the specific mechanism of RHBDF1 regulating the biological behaviors of SCLC, RHBDF1 and its co-expressed genes from our previous RNA sequencing results in SCLC [5,6] were performed for functional enrichment analysis. Gene ontology (GO) analysis showed that RHBDF1 was mainly involved in various biological processes (BP), including RNA splicing, nuclear transport, RNA localization, protein acylation, and dephosphorylation (Fig. S3A); cellular components (CC) including spliceosomal complex, proteasome complex, ubiquitin ligase complex, site of DNA damage, ATPase complex (Fig. S3B); molecular function (MF), including translation factor activity, proteasome binding, ubiquitin-protein transferase activity, translation regulator activity (Fig. S3C). Moreover, Kyoto Encyclopedia of Genes and Genomes (KEGG) enrichment analysis suggested that RHBDF1 was mainly involved in the

spliceosome, proteasome, and ubiquitin-mediated proteolysis (Fig. S3D).

3.4. RHBDF1 regulated cell proliferation and cisplatin sensitivity by YAP1/Smad2 pathway

According to the STRING database, YAP1 and Smad2/3/4 potentially interacted with RHBDF1, which garnered our attention (Fig. 2A). To determine that YAP1 and Smad2 were involved in the role of RHBDF1 effects in cell proliferation and cisplatin sensitivity, we determined the expression of YAP1 and Smad2 by qRT-PCR and western blotting. The results showed that RHBDF1 overexpression leads to YAP1 downregulation (Fig. 2B and C), whereas RHBDF1 knockdown leads to YAP1 upregulation (Fig. 2D and E), which was parallel with a stable expression of Smad2 (data not shown). Next, the interaction of RHBDF1, YAP1, and Smad2 was determined by IP, in which we detected binds of YAP1 and Smad2 after IP using an anti-Flag-RHBDF1 antibody (Fig. 2F), and binds of RHBDF1 and Smad2 after IP using an anti-YAP1 antibody (Fig. 2G). The interactions among the three proteins were successfully validated. Western
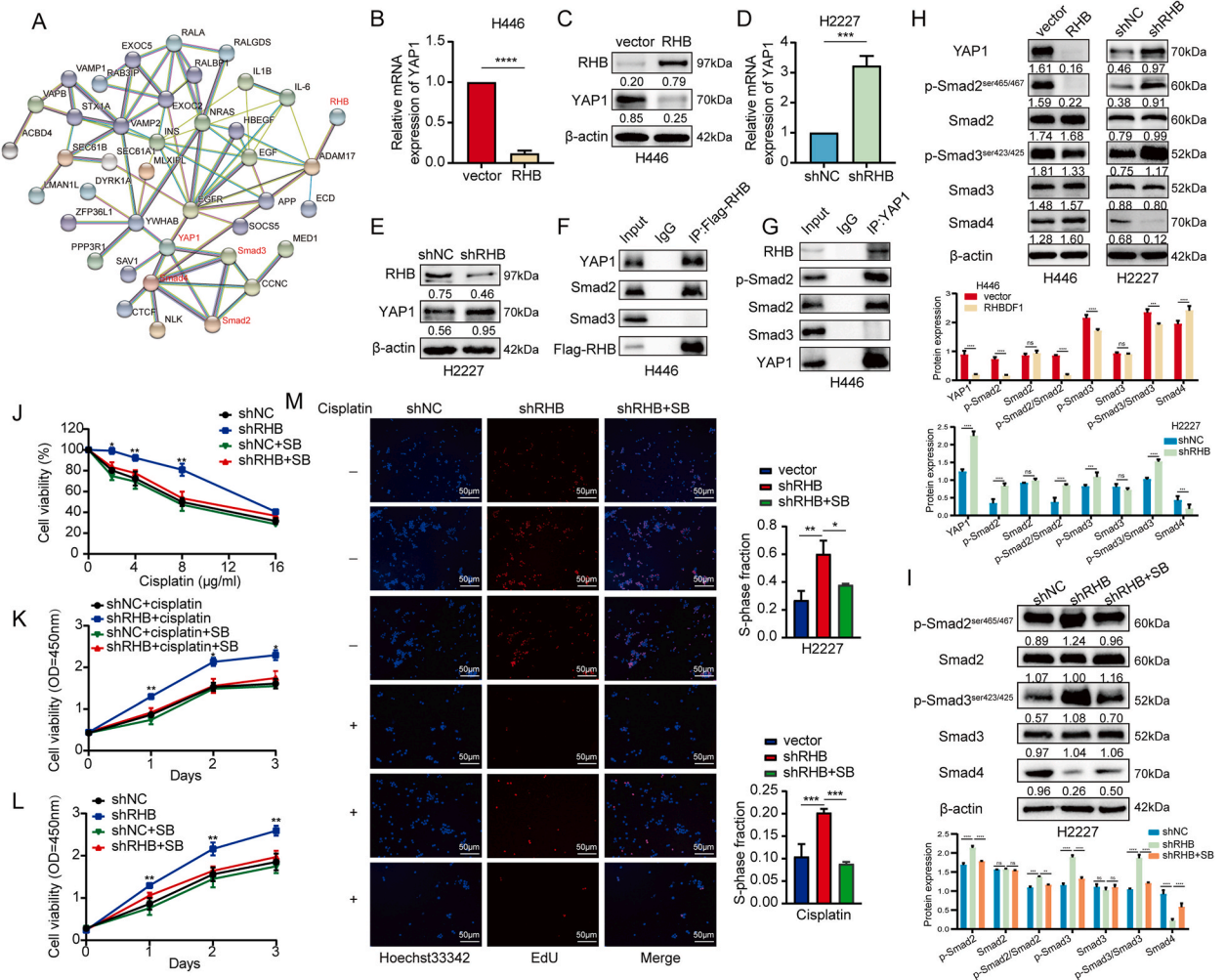
Fig. 2. RHBDF1 inhibited cell proliferation and enhanced cisplatin sensitivity by YAP1/Smad2 pathway. (A) Protein–protein interaction (PPI) network was constructed by STRING. The mRNA and protein levels of YAP1 were determined in RHBDF1-overexpressing cells by qRT-PCR (vector was normalized to 1) (B) and western blotting (C). The mRNA and protein levels of YAP1 were detected in RHBDF1 knockdown cells by qRT-PCR (shNC was normalized to 1) (D) and western blotting (E). (F) IP experiments validated the interaction of RHBDF1 with YAP1 and Smad2. (G) IP experiments validated the interaction of YAP1 with RHBDF1 and Smad2. (H) Western blotting was conducted to explore the expression of YAP1, p-Smad2, p-Smad3, and Smad4 in H446-RHB and H2227-shRHB cells. (I) Western blotting was performed to analysis YAP1, p-Smad2, p-Smad3, and Smad4 in H2227 knockdown cells compared to control cells with or without 10 μM SB431542 for 2 h. (J) Cell viability of H2227-shRHBDF1 cells after incubation with the indicated concentrations of cisplatin for 24 h in the presence of 10 μM SB431542 for 72 h was evaluated by a CCK-8 assay. Additional CCK-8 assay was used to observe changes in the proliferation rate of H2227-shRHBDF1 cells cultured with (K) or without (L) 0.5 μg/mL cisplatin for 24 h either alone or in combination with 10 μM SB431542 for 72 h. (M) An EdU incorporation assay was performed to detect cell viability in H2227-shRHBDF1 cells with or without cisplatin in the presence or absence of SB431542. β-actin was normalized to 1 in western blotting. N = 3 technical replicates, experiment was repeated at least 3 times. (*p < 0.05, **p < 0.01, ***p < 0.001, ****p < 0.0001).

blotting analysis showed that the levels of YAP1, phosphorylation of Smad2 and Smad3 were decreased, whereas the level of Smad4 expression was increased in H446-RHB cells. On the contrary, the opposite phenomena were observed in H2227-shRHB cells (Fig. 2H). To investigate the critical role of the Smad2/3 pathway in RHBDF1 mediated biological function, H2227-shRHB cells were treated with 10 μM SB431542, a phosphorylation inhibitor of Smad2/3, for 2 h. The inhibition of Smad2/3 phosphorylation was investigated with the whole cell lysates and presented in Fig. 2I. As shown in Fig. 2I, RHBDF1 knockdown elicited increased phosphorylation of Smad2/3, and downregulated expression of Smad4 can be substantially reversed after SB431542 treatment. RHBDF1 knockdown desensitized H2227 cells to cisplatin, which can be fully rescued after treatment with 10 μM SB431542 for 72 h (Fig. 2J). Moreover, CCK-8 and EdU assays showed that RHBDF1 knockdown increased the viability of H2227 cells in treatment with or without cisplatin, the effect was reversed when SB431542 was introduced (Fig. 2K–M). The above findings collectively suggested that RHBDF1 regulated cell proliferation and cisplatin sensitivity through the YAP1/Smad2 signaling pathway *in vitro*.
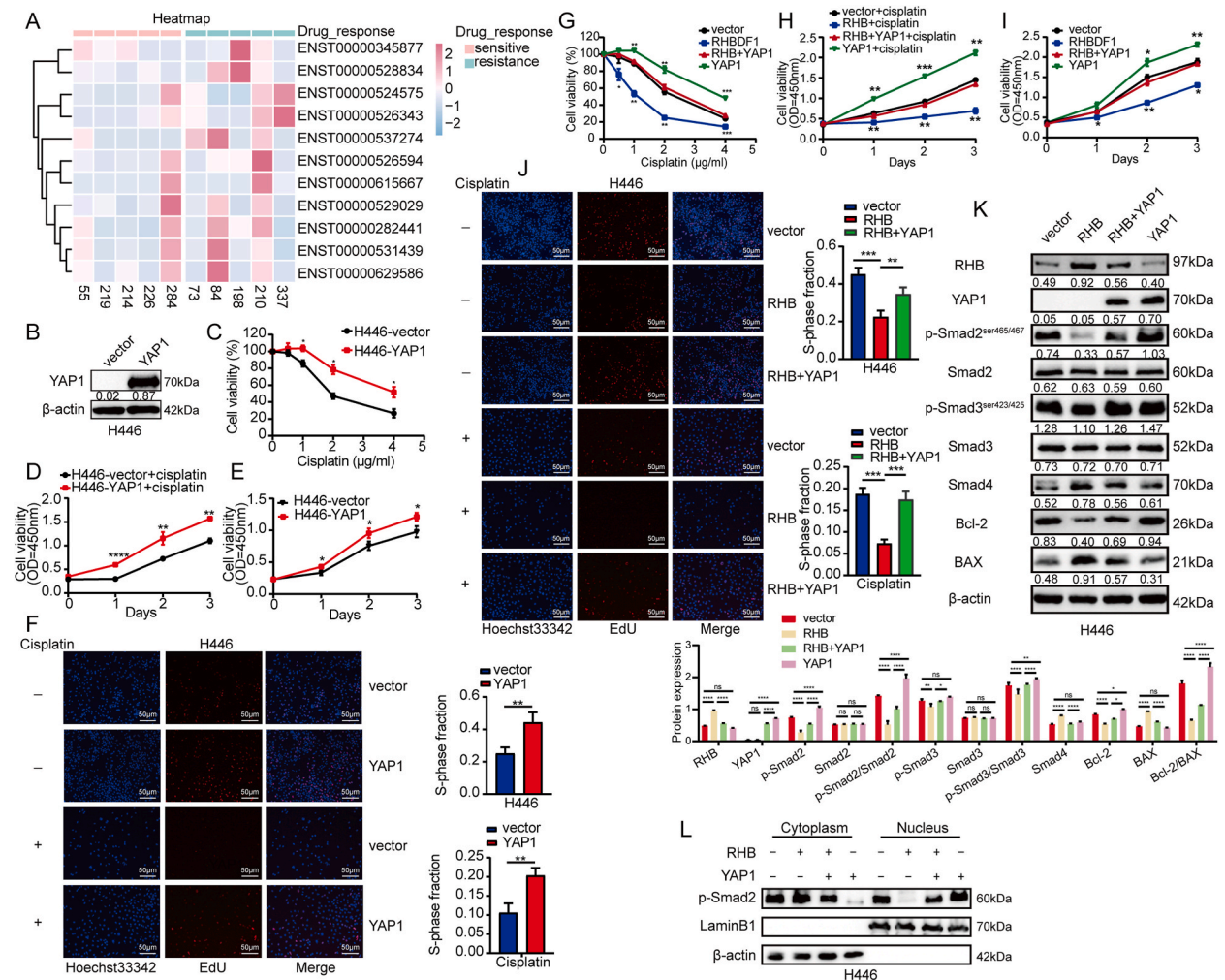

Fig. 3. YAP1 overexpression reversed the functional phenotypes of RHBDF1. (A) Heat map illustrating the differential expression of 11 YAP1 transcripts in 5 intrinsic cisplatin-resistant SCLC tissues and 5 intrinsic cisplatin-sensitive SCLC tissues. (B) Western blotting was used to verify the protein levels of YAP1 in H446 cells after stably transfected with pCMV-zsG-Puro-YAP1 recombinant vector or pCMV-zsG-Puro vector. (C) H446-YAP1 and corresponding control cells were treated with the indicated concentration of cisplatin for 24 h, and cell viability was performed by a CCK-8 assay. Cell proliferation was analyzed by a CCK-8 assay (D–E) and an EdU assay (F) in YAP1-overexpressing H446 cells with or without 0.5 μg/mL cisplatin treatment for 24 h. (G) Cell viability of H446 cells in respond to overexpression of RHBDF1 and/or YAP1 with the concentration gradients of cisplatin for 24 h was evaluated by a CCK-8 assay. A CCK-8 assay (H–I) and an EdU incorporation assay (J) was conducted to determine the cell proliferation of H446 cells in respond to overexpression of RHBDF1 and/or YAP1 with or without cisplatin treatment. (K) Western blotting was used to evaluate YAP1, p-Smad2, p-Smad3, Smad4 and apoptosis-related markers of H446 cells in respond to overexpression of RHBDF1 and/or YAP1. (L) The expression levels of p-Smad2 in the cytoplasm and nucleus were analyzed by subcellular fractionation assays in H446 cells. β-actin was used as the control for cytoplasmic protein, while Lamin B1 was used as the control for nuclear protein. β-actin was normalized to 1 in western blotting. N = 3 technical replicates, experiment was repeated at least 3 times. (*p < 0.05, **p < 0.01, ***p < 0.001, ****p < 0.0001).

3.5. YAP1 overexpression reversed the functional phenotypes of RHBDF1

We determined our previous RNA sequencing results [5,6] and found that YAP1 was highly expressed in drug-resistant patients with SCLC compared with drug-sensitive patients with SCLC (Fig. 3A). Considering the results of RNA sequencing and the importance of YAP1 in the chemoresistance and tumorigenesis of SCLC, we overexpressed YAP1 in H446 via plasmid transfection and validated the expression with western blotting (Fig. 3B). YAP1 overexpression desensitized H446 cells to cisplatin (Fig. 3C). Moreover, CCK-8 and
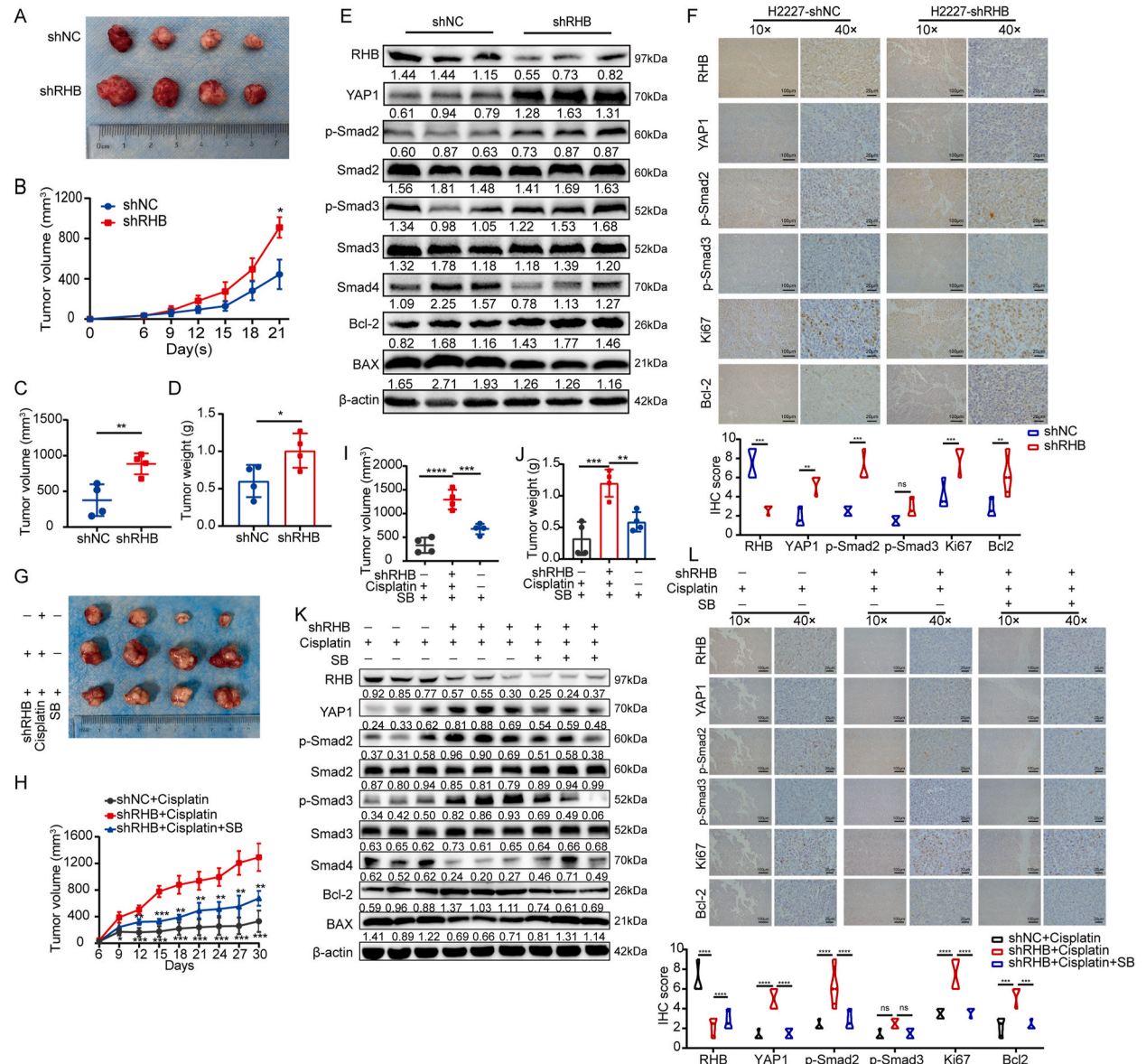
Fig. 4. RHBDF1 inhibited cell proliferation and enhanced cisplatin sensitivity via YAP1/Smad2 signaling, which SB431542 could partially reverse *in vivo*. (A) Representative images of tumors in nude mice at the end timepoint. (B) Line chart of tumor volume during follow-up for 21 days. (C) Scatter diagram of the final tumor volumes. (D) Histogram of the final tumor weights. (E) Western blotting was used to analyze the protein expression of YAP1, p-Smad2, p-Smad3, Smad4 and apoptosis-related markers in tissues obtained from harvested tumors. (F) IHC was conducted to confirm the expression of RHBDF1, YAP1, p-Smad2, p-Smad3, Ki67, and Bcl-2 in the tumor samples. Magnification, $\times$ 100 and $\times$ 400. (G) Representative images of tumors in nude mice at the end timepoint from the three groups: (1) H2227-shNC + cisplatin + vehicle, (2) H2227-shRHB + cisplatin + vehicle, (3) H2227-shRHB + cisplatin + SB431542. (H) Line chart of tumor volume during follow-up for 30 days in the three groups. (I) Scatter diagram of the final tumor volumes in the three groups. (J) Histogram of the final tumor weights in the three groups. (K) Western blotting was used to evaluate the protein expression of YAP1, p-Smad2, p-Smad3, Smad4 and apoptosis-related markers in tumor tissues obtained from three groups. (L) IHC was conducted to confirm the expression of RHBDF1, YAP1, p-Smad2, p-Smad3, Ki67, and Bcl-2 in the three groups of tumor samples. Magnification, $\times$ 100 and $\times$ 400. β-actin was normalized to 1 in western blotting. (*$p < 0.05$, **$p < 0.01$, ***$p < 0.001$, ****$p < 0.0001$).
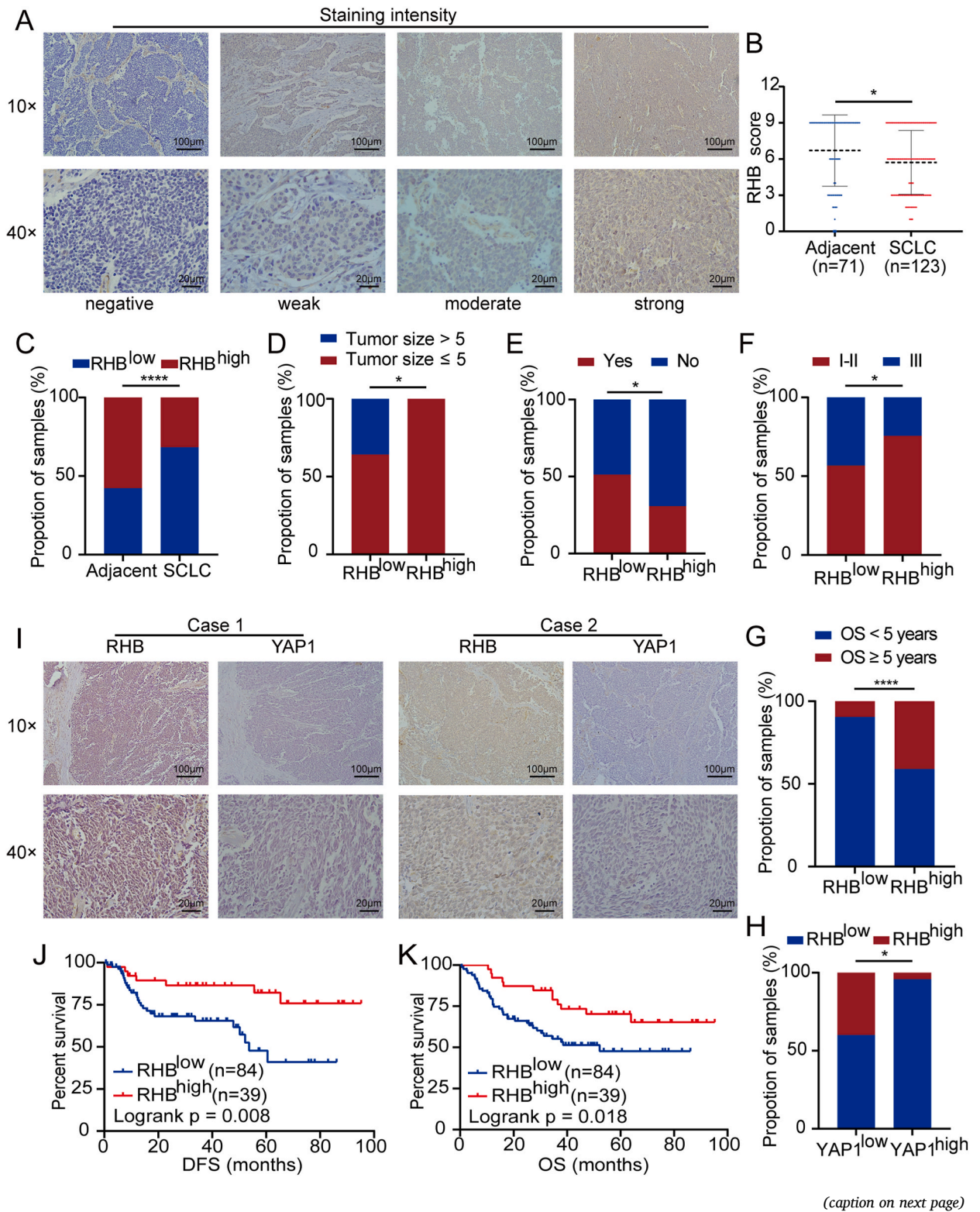
Fig. 5. RHBDF1 was low expressed in SCLC and was associated with clinicopathological features. (A) Representative IHC images of different expression intensities of RHBDF1 in SCLC tissues were displayed with original magnification, × 100, × 400, respectively. (B) RHBDF1 expression score in SCLC tissues compared with adjacent lung tissues by IHC. (C) Proportion of RHBDF1 expression in SCLC tissues and adjacent lung tissues. Proportion of tumor size (D), lymph node metastasis (E), TNM stage (F) in low- and high- RHBDF1 expression groups. Proportion of RHBDF1 expression in OS greater than or less than 5 years (G), or low- and high- YAP1 expression groups (H). (I) Representative images of two SCLC tumor tissues with greater RHBDF1 expression but less YAP1 expression. Magnification, × 100 and × 400. The correlation between RHBDF1 expression and DFS (J) and OS (K) in SCLC patients. (*p < 0.05, ****p < 0.0001).

EdU assays showed that YAP1 overexpression increased the viability of H446 cells in the presence or absence of cisplatin (Fig. 3D–F). Furthermore, the overexpression of YAP1 in H446-RHB cells effectively restored RHBDF1-mediated cell proliferation and cisplatin sensitivity (Fig. 3G–J). During the same time, the Smad2 signaling cassette was also restored (Fig. 3K). Previous studies have shown that YAP1 could promote the nuclear translocation of Smad2 [16,25]. In this study, cytosolic and nuclear proteins were isolated from H446-YAP1 cells. As shown in Fig.3L, we observed that more p-Smad2 accumulated in the nucleus of H446-YAP1 cells, whereas less p-Smad2 was retained in the cytoplasm, suggesting that YAP1 promotes the nuclear translocation of Smad2. Conversely, more p-Smad2 accumulated in the cytoplasm and less p-Smad2 was retained in the nucleus of H446-RHB cells, indicating that RHBDF1 inhibits p-Smad2 translocation into the nucleus. Our data suggested that YAP1 could reverse the functional phenotypes of RHBDF1 by the Smad2 signaling pathway in SCLC.

3.6. RHBDF1 regulated cell proliferation and cisplatin sensitivity via YAP1/Smad2 signaling, which SB431542 could partially reverse in vivo

RHBDF1 stably knocked-down H2227 cells were subcutaneously inoculated into the left axilla of nude mice. As shown in Fig. 4A, RHBDF1 knockdown promoted tumor proliferation by 42.53 % during the follow-up. Tumor volumes and weights in the shRHB group were greater than those in the shNC group (fold changes = 2.35 and 1.68, respectively, Fig. 4B–D). The western blotting of total protein isolated from tumor tissues of 3 mice in each group showed that the levels of YAP1 and Bcl-2 as well as the phosphorylation of Smad2 and Smad3 were increased, whereas the expressions of Smad4 and BAX were decreased (Fig. 4E). Moreover, the levels of YAP1, Ki67, and Bcl-2 as well as the phosphorylation of Smad2 and Smad3 were evaluated by IHC (Fig. 4F). These results strongly indicated that RHBDF1 downregulation induced proliferation via the YAP1/Smad2 signaling pathway in vivo.

To further verify the regulatory effect of RHBDF1 on cisplatin sensitivity in vivo, BALB/c-nu mice were subcutaneously injected with H2227 cells with or without RHBDF1 depletion into the left axilla and randomized into three groups: (1) H2227-shNC + cisplatin + vehicle, (2) H2227-shRHB + cisplatin + vehicle, and (3) H2227-shRHB + cisplatin + SB431542. Increased tumor burden was observed in the RHBDF1-silenced H2227 cells treated with cisplatin compared with that in the H2227-shNC cells (Fig. 4G–J), suggesting that RHBDF1 mediated cisplatin sensitivity in vivo. In addition, treatment with cisplatin + SB431542 partially reduced tumor burden elicited by RHBDF1 depletion compared with that in mice treated with cisplatin alone (Fig. 4G–J). These results strongly indicated that SB431542 could reverse the effect of RHBDF1-mediated cisplatin sensitivity in vivo. The Western blot analysis suggested that the levels of YAP1 and Bcl-2, as well as the phosphorylation of Smad2 and Smad3, were increased, whereas the expressions of Smad4 and BAX were decreased in the RHBDF1-silenced H2227 tumors than in the control tumors treated with cisplatin (Fig. 4K). Importantly, the expression signatures of these genes could be restored by SB431542 treatment (Fig. 4K), which was further confirmed by IHC (Fig.4L). These results strongly indicated that RHBDF1 played a crucial role in cisplatin sensitivity and mediated cisplatin sensitivity via the YAP1/Smad2 pathway in vivo.

3.7. RHBDF1 was low expressed in SCLC and was associated with clinicopathological features

To elucidate the clinical significance of RHBDF1 in SCLC, tumor tissues (n = 123) and adjacent lung tissues (n = 71) were collected to examine RHBDF1 expression. IHC results suggested that RHBDF1 was mainly expressed in the cytoplasm of the tumor cells (Fig. 5A). RHBDF1 expression was significantly reduced in the SCLC tissues than in the adjacent lung tissues (Fig. 5B, p = 0.017). According to the Clinical and Laboratory Standards Institute guidelines [26–28], the optimal cutoff ratio (7.5) was taken from the receiver-operating characteristic curve analysis of the SCLC tissues and adjacent lung tissues. The patients were divided into high- and low-RHBDF1 expression groups based on this cutoff value with the best sensitivity and specificity and then quantitative analysis showed that RHBDF1 expression was decreased in a greater portion of the SCLC tissues (84/123, 68.29 %) than in the adjacent lung tissues (30/71, 42.25 %) (Fig. 5C–Table S3, p < 0.0001). Furthermore, the relationship between RHBDF1 and clinicopathological features was analyzed. The results showed that RHBDF1 was correlated with tumor size (Fig. 5D, p = 0.029), lymph node metastasis (Fig. 5E, p = 0.034), TNM stage (Fig. 5F, p = 0.031), and 5-year survival (Fig. 5G, p = 0.0001), whereas was unrelated to gender, age, smoking history, T stage, and pleural invasion (Table 1). Moreover, YAP1 expression was detected by IHC, the results suggested that YAP1 was expressed in both the cytosol and nucleus of tumor cells and the positive expression rate was 27.64 % (34/123).However, spearman analysis showed that RHBDF1 and YAP1 expressions were negatively correlated without any statistically significant difference (data not shown). Further analysis showed that RHBDF1 was downregulated in tissues with high YAP1 expression (Fig. 5H–I, p = 0.019). Furthermore, the high RHBDF1 expression group showed better disease-free survival (DFS) (Fig. 5J, p = 0.005) and OS (Fig. 5K, p = 0.018) than the low RHBDF1 expression group by the KM analysis. Using the COX hazard regression model for univariate and multivariate analyses, the univariate analysis showed that lymph node metastasis (Table S4, p = 0.015) and RHBDF1 expression (Table S4, p = 0.011) were associated with DFS, whereas T stage (Table S5, p = 0.024), lymph node metastasis (Table S5, p = 0.001),

TNM stage (Table S5, p = 0.0001), and RHBDF1 expression (Table S5, p = 0.021) were associated with OS. The multivariate analysis showed that RHBDF1 expression (Table S4, p = 0.034) was an independent prognostic factor for DFS. Furthermore, TNM stage (Table S5, p = 0.002) and RHBDF1 expression (Table S5, p = 0.045) were independent prognostic factors for OS.

4. Discussion

Platinum-based chemotherapy is the mainstay therapy for SCLC, and chemoresistance has been a major challenge over the past several decades [29]. The specific molecular mechanism underlying SCLC chemoresistance is still not completely understood. In the present study, we identified a chemosensitivity-relevant gene, RHBDF1. Our data revealed a novel molecular mechanism involving RHBDF1, YAP1 and Smad2 signaling in regulating SCLC chemoresistance and progression. Specifically, RHBDF1 could interact with YAP1, regulating YAP1 expression at transcriptive and protein levels. YAP1 upregulation enhanced Smad2 nuclear translocation, leading to the activation of downstream target genes Bcl-2 and BAX.

Based on our previous gene profiling, using several GEO databases, we explored DEGs between the SCLC and adjacent lung tissues and verified that RHBDF1 was downregulated in SCLC and was associated with OS. Then, we explored the biological functions of RHBDF1 *in vitro* and *in vivo*. We found that RHBDF1 expression was lower in the SCLC cells than that in the normal cells, the forced expression of RHBDF1 inhibited cell proliferation and promoted apoptosis and cisplatin sensitivity in the SCLC cells, and the depletion of RHBDF1 elicited opposite phenomena. Moreover, the tumor volumes and weights were increased in the RHBDF1-silenced H2227 tumor model in the presence or absence of cisplatin. These results indicated that RHBDF1 might play an important role in regulating SCLC cell proliferation and cisplatin sensitivity *in vivo*, which were consistent with the results *in vitro*. Previous studies have shown the cancer-promoting function of RHBDF1 in head and neck squamous carcinoma, breast cancer, colorectal cancer, and cervical cancer [2, 4,9–11,30–35]. The reason behind the opposite results might be partial because of a difference in the genetic signatures, the tumor stroma, or the tumor microenvironment of these different tumors.

The functional enrichment analysis of RHBDF1 and its co-expressed genes was performed using our previous RNA sequencing data [5,6]. We found that RHBDF1 was related to proteasome and ubiquitination. Studies have demonstrated that cell proliferation is regulated by the ubiquitin–proteasome pathway. Cathepsin K promotes the proliferation of hepatocellular carcinoma cells through induction of SIAH1 ubiquitination and degradation [36]. CUL5-ASB6 complex promotes p62/SQSTM1 ubiquitination and degradation to regulate cell proliferation and autophagy. Based on functional enrichment analysis, we reasonable speculate that RHBDF1 may regulates cell proliferation by regulating proliferation-related proteins through ubiquitin–proteasome pathway. This is a very

Table 1
Correlation between RHBDF1 expression and clinicopathological characteristics of patients with SCLC.

Variables	RHBDF1 expression		Total	χ^2	p-value
	Low	High			
Age (year)				0.075	0.784
≤60	43	21	64		
>60	41	18	59		
Gender				0.087	0.768
Female	30	15	45		
Male	54	24	78		
Smoke				2.703	0.1
No	32	9	41		
Yes	52	30	82		
Tumor size (cm)				5.331	0.029*
≤5	68	38	106		
>5	10	0	10		
null			7		
T stage				4.803	0.187
T1	41	25	66		
T2	29	8	37		
T3	4	0	4		
T4	10	5	15		
null			1		
Lymph node metastasis				4.493	0.034*
Yes	43	12	55		
No	41	27	68		
TNM stage				4.647	0.031*
I -II	25	19	44		
III	59	19	78		
null			1		
Pleural invasion				0.001	0.982
Yes	24	11	35		
No	54	25	79		
5 years survival				16.83	0.0001*
Yes	8	16	24		
No	76	23	99		

interesting direction in the following study.

PPI network results suggested that RHBDF1 might interact with YAP1 and Smad2. In our study, we have observed the interactions among the RHBDF1 and YAP1 and Smad2 in co-immunoprecipitations, but there were no obvious interactions either between Smad3 and RHBDF1 or between Smad3 and YAP1, indicating that RHBDF1 directly regulated Smad2 rather than Smad3 to exert biologic function. As shown in Fig. 2H-I, we observed that there were both a significance change of Smad2 phosphorylation and Smad3 phosphorylation in H2227 cells, while in H446 cells, Smad2 phosphorylation had a more drastic change than Smad3 phosphorylation. What's more, as shown in Fig. 4F and L, IHC results indicated that there was no statistical difference in Smad3 phosphorylation *in vivo*. Therefore, the phosphorylation of Smad2 plays a more significant role in RHBDF1 regulation of biological function, while Smad3 may have other unknown regulatory pathways in H2227 cells. We believe that the phenomenon observed in our study may be related with the complexity of the signaling dynamics involved. Most importantly, the Co-IP results demonstrated that RHBD1 interacts with Smad2 but not SMAD3. What's more, miR-486-5p regulated cisplatin sensitivity of human muscle-invasive bladder cancer cells by induction of apoptosis though Smad2 [37]. MiR-10a mediated cisplatin resistance in lung cancer cell line via the transforming growth factor-β/Smad2/STAT3/STAT5 pathway [38]. In light of this, we primarily focused on phosphorylated Smad2 because our preliminary data and several studies suggested that Smad2 plays a more significant role in the cisplatin sensitivity. The nuclear accumulation of the hippo signaling transducers YAP1/TEA domain family member in human EGFR2-positive breast cancer results in acquired trastuzumab resistance [39]. YAP1 overexpression also induced drug resistance to 5-fluorouracil and docetaxel by increasing EGFR expression in esophageal cancer [40], and YAP1 activation was associated with a poor prognosis and cetuximab resistance in colorectal cancer [41]. As a target gene of miR-630, YAP1 responds to EGFR-TKI therapy unfavorably via the miR-630/YAP1/ERK feedback loop in EGFR-mutation lung adenocarcinomas [35]. These results suggested that YAP1 was associated with drug resistance in various tumors. Growing evidence suggested that the TGF-β/Smad signaling pathway was crucial for chemotherapy drug resistance. Curcumin reversed oxaliplatin resistance by regulating the TGF-β/Smad2/3 signaling pathway in colorectal cancer [42]. FAM46A overexpression induced cisplatin resistance by activating TGF-β/Smad2 signaling and upregulating nuclear Smad2 expression in ovarian cancer [43]. MicroRNA-552 knockdown mediated 5-fluorouracil resistance via the Smad2 pathway in colorectal cancer [29,44]. In our study, the high basal levels of Smad2/3 phosphorylation without TGF-β maybe suggest that phosphorylated Smad2/3 is associated with the development and progression of SCLC. A study revealed that the phosphorylated Smad2 expression appeared in the nuclei and in the cytoplasm of liver cells and it was positively correlated with the severity of the tumor pathology. The aberrant expressions of phosphorylated Smad2 may play an important role in the pathogenesis of hepatocellular carcinoma [45]. Smad2 and Smad3 phosphorylated transmit malignant TGF-β signal in later stages of human colorectal cancer [46]. Using human breast cancer tissue microarrays, Liu et al. suggested that Smad3 linker phosphorylation promotes tumorigenesis but inhibits metastasis [47]. Importantly, YAP1 regulated TGF-β transcriptional activity and Smad2 phosphorylation in lung cancer cells [48]. The high expression of YAP1 was significantly correlated with Smad2 nuclear localization [25], and RASSF1A degradation promoted YAP1 association with Smad2 and its subsequent nuclear translocation [16]. We, for the first time, showed that RHBDF1 interacted with YAP1 and contributed to Smad2 nuclear translocation in SCLC in the present study.

Previous study showed that RHBDF1 was highly expressed in colorectal cancer patients and was associated with poor OS [10,11]. RHBDF1 mRNA levels in breast cancer specimens was higher than that in the normal breast tissues [30,49]. Another study, on breast cancer, suggested that RHBDF1 expression was elevated in tumor tissues and was correlated with poor prognosis [9]. Furthermore, RHBDF1 was low expressed in the high YAP1 expression group, suggesting a negative correlation between the two molecules. However, Spearman correlation analysis between RHBDF1 and YAP1 showed no statistical significance. This might be because, among the 123 samples of SCLC tissues, only 34 (27.64 %) were positive for YAP1 by IHC. The study showed that the positive rates of YAP1 expression in combined and pure SCLCs were 52.17 % (24/46) and 29.10 % (73/251), respectively, in postoperative patients [50]. Song et al. showed that 26.42 % (14/53) of patients wi ·th SCLC were YAP1 positive [13]. A further study found that the positive rate of YAP1 phosphorylation was 21.62 % (8/37) in patients with SCLC [28]. Therefore, the small sample size of patients was also the major limitation of this study, although we firstly clarified that high RHBDF1 expression showed better DFS and OS, and RHBDF1 was an independent prognostic factor for DFS and OS in SCLC.

We are the first to reveal that RHBDF1 regulated cell proliferation and cisplatin sensitivity in SCLC by interacting with YAP1, facilitating Smad2 translocation to the nucleus. These findings provided a more comprehensive understanding of the specific mechanisms of chemoresistance in SCLC. Blocking this pathway may be a potential therapeutic strategy to increase the effectiveness of cisplatin in patients with SCLC.

Ethical approval and consent to participate

All clinical samples were from the Harbin Medical University Cancer Hospital. The study has been carried out in accordance with the World Medical Association Declaration of Helsinki, and informed consent waivers were granted by the Ethics Committee at Harbin Medical University Cancer Hospital. All animal work was performed at the Second Affiliated Hospital of Harbin Medical University and complied with the Institutional Animal Care and Use Committee (IACUC) and the NIH Guide for the Care and Use of Laboratory Animals. All human specimens and relevant experimental procedures in nude mice were collected in accordance with the protocol approved by the Ethics Committee at Harbin Medical University Cancer Hospital (approval number: KY2021-15, dated: April 23, 2021).

Funding

Data availability statement

All supporting data are included within the article and its additional files. All the raw data was uploaded on Jianguoyun/Nutstore. https://www.jianguoyun.com/p/DWWjBDkQsYCyCxiFnPUEIAAT.

CRediT authorship contribution statement

Lei Wang: Writing – original draft, Visualization, Investigation, Formal analysis, Data curation. **Lishuang Qi:** Visualization, Software, Formal analysis. **Xiaoyi Huang:** Writing – review & editing, Project administration. **Xiao Feng:** Validation, Investigation. **Junqing Gan:** Validation, Investigation. **Juxuan Zhang:** Visualization, Software. **Yuhui Xi:** Writing – review & editing. **Shuai Zhang:** Resources. **Qingwei Meng:** Writing – review & editing, Supervision, Resources, Project administration, Funding acquisition, Conceptualization.

Declaration of competing interest

The authors declare that they have no known competing financial interests or personal relationships that could have appeared to influence the work reported in this paper.

Acknowledgements

Appendix A. Supplementary data

Supplementary data to this article can be found online at https://doi.org/10.1016/j.heliyon.2024.e33454.

References

[1] R.Y. Tay, F. Fernández-Gutiérrez, V. Foy, K. Burns, J. Pierce, K. Morris, et al., Prognostic value of circulating tumour cells in limited-stage small-cell lung cancer: analysis of the concurrent once-daily versus twice-daily radiotherapy (CONVERT) randomised controlled trial, Ann. Oncol. 30 (7) (2019) 1114–1120.

[2] P. Ponath, D. Menezes, C. Pan, B. Chen, M. Oyasu, D. Strachan, et al., A novel, fully human anti-fucosyl-GM1 antibody demonstrates potent in vitro and in vivo antitumor activity in preclinical models of small cell lung cancer, Clin. Cancer Res. 24 (20) (2018) 5178–5189.

[3] X. Chen, N. Amar, Y. Zhu, C. Wang, C. Xia, X. Yang, et al., Combined DLL3-targeted bispecific antibody with PD-1 inhibition is efficient to suppress small cell lung cancer growth, Journal for immunotherapy of cancer 8 (1) (2020).

[4] Q. Xu, C. Chen, B. Liu, Y. Lin, P. Zheng, D. Zhou, et al., Association of iRhom1 and iRhom2 expression with prognosis in patients with cervical cancer and possible signaling pathways, Oncol. Rep. 43 (1) (2020) 41–54.

[5] R. Ji, Q. Shi, Y. Cao, J. Zhang, C. Zhao, H. Zhao, et al., Alternative splicing of the human rhomboid family-1 gene RHBDF1 inhibits epidermal growth factor receptor activation, J. Biol. Chem. 298 (6) (2022) 102033.

[6] J. Zhang, J. Deng, X. Feng, Y. Tan, X. Li, Y. Liu, et al., Hierarchical identification of a transcriptional panel for the histological diagnosis of lung neuroendocrine tumors, Front. Genet. 13 (2022) 944167.

[7] L. Deng, J. Zou, Y. Su, M. Wang, L. Zhao, Resveratrol inhibits TGF-β1-induced EMT in gastric cancer cells through Hippo-YAP signaling pathway, Clin. Transl. Oncol. 24 (11) (2022) 2210–2221.

[8] A. Mondal, J. Roberge, J. Gilleran, Y. Peng, D. Jia, M. Akel, et al., Bone morphogenetic protein inhibitors and mitochondria targeting agents synergistically induce apoptosis-inducing factor (AIF) caspase-independent cell death in lung cancer cells, Cell Commun. Signal. 20 (1) (2022) 99.

[9] Z. Zhou, F. Liu, Z.S. Zhang, F. Shu, Y. Zheng, L. Fu, et al., Human rhomboid family-1 suppresses oxygen-independent degradation of hypoxia-inducible factor-1α in breast cancer, Cancer Res. 74 (10) (2014) 2719–2730.

[10] J. Li, T.R. Bai, S. Gao, Z. Zhou, X.M. Peng, L.S. Zhang, et al., Human rhomboid family-1 modulates clathrin coated vesicle-dependent pro-transforming growth factor α membrane trafficking to promote breast cancer progression, EBioMedicine 36 (2018) 229–240.

[11] H. Yuan, R. Wei, Y. Xiao, Y. Song, J. Wang, H. Yu, et al., RHBDF1 regulates APC-mediated stimulation of the epithelial-to-mesenchymal transition and proliferation of colorectal cancer cells in part via the Wnt/β-catenin signalling pathway, Exp. Cell Res. 368 (1) (2018) 24–36.

[12] C.M. Rudin, J.T. Poirier, L.A. Byers, C. Dive, A. Dowlati, J. George, et al., Molecular subtypes of small cell lung cancer: a synthesis of human and mouse model data, Nat. Rev. Cancer 19 (5) (2019) 289–297.

[13] Y. Song, Y. Sun, Y. Lei, K. Yang, R. Tang, YAP1 promotes multidrug resistance of small cell lung cancer by CD74-related signaling pathways, Cancer Med. 9 (1) (2020) 259–268.

[14] R. Tang, Y. Lei, B. Hu, J. Yang, S. Fang, Q. Wang, et al., WW domain binding protein 5 induces multidrug resistance of small cell lung cancer under the regulation of miR-335 through the Hippo pathway, Brit j cancer 115 (2) (2016) 243–251.

[15] K. Grannas, L. Arngården, P. Lönn, M. Mazurkiewicz, A. Blokzijl, A. Zieba, et al., Crosstalk between hippo and TGFβ: subcellular localization of YAP/TAZ/Smad complexes, J. Mol. Biol. 427 (21) (2015) 3407–3415.

[16] D.E. Pefani, D. Pankova, A.G. Abraham, A.M. Grawenda, N. Vlahov, S. Scrace, et al., TGF-B targets the hippo pathway scaffold RASSF1A to facilitate YAP/SMAD2 nuclear translocation, Mol. Cell 63 (1) (2016) 156–166.

[17] G. Zhou, O. Soufan, J. Ewald, R.E.W. Hancock, N. Basu, J. Xia, NetworkAnalyst 3.0: a visual analytics platform for comprehensive gene expression profiling and meta-analysis, Nucleic Acids Res. 47 (W1) (2019) W234–w241.

[18] D. Szklarczyk, A.L. Gable, K.C. Nastou, D. Lyon, R. Kirsch, S. Pyysalo, et al., The STRING database in 2021: customizable protein-protein networks, and functional characterization of user-uploaded gene/measurement sets, Nucleic Acids Res. 49 (D1) (2021) D605–d612.

[19] Z. Jiao, X. Feng, Y. Cui, L. Wang, J. Gan, Y. Zhao, et al., Expression characteristic, immune signature, and prognosis value of EFNA family identified by multi-omics integrative analysis in pan-cancer, BMC Cancer 22 (1) (2022) 871.

[20] L. Wang, X. Feng, Z. Jiao, J. Gan, Q. Meng, Characterization of the prognostic and diagnostic values of ALKBH family members in non-small cell lung cancer, Pathol. Res. Pract. 231 (2022) 153809.

[21] L. Cai, H. Liu, F. Huang, J. Fujimoto, L. Girard, J. Chen, et al., Cell-autonomous immune gene expression is repressed in pulmonary neuroendocrine cells and small cell lung cancer, Commun. Biol. 4 (1) (2021) 314.

[22] L. Jiang, J. Huang, B.W. Higgs, Z. Hu, Z. Xiao, X. Yao, et al., Genomic landscape survey identifies SRSF1 as a key oncodriver in small cell lung cancer, PLoS Genet. 12 (4) (2016) e1005895.

[23] S. Kastner, T. Voss, S. Keuerleber, C. Gl?ckel, M. Freissmuth, W. Sommergruber, Expression of G protein-coupled receptor 19 in human lung cancer cells is triggered by entry into S-p hase and supports G(2)-M cell-cycle progression, Mol. Cancer Res. 10 (10) (2012) 1343–1358.

[24] J. George, J.S. Lim, S.J. Jang, Y. Cun, L. Ozretić, G. Kong, et al., Comprehensive genomic profiles of small cell lung cancer, Nature 524 (7563) (2015) 47–53.

[25] K. Sugimachi, M. Nishio, S. Aishima, Y. Kuroda, T. Iguchi, H. Komatsu, et al., Altered expression of hippo signaling pathway molecules in intrahepatic cholangiocarcinoma, Oncology-basel 93 (1) (2017) 67–74.

[26] H. Hautzel, O. Sander, A. Heinzel, M. Schneider, H.W. Miller, Assessment of large-vessel involvement in giant cell arteritis with 18F-FDG PET: introducing an ROC-a nalysis-based cutoff ratio, J. Nucl. Med. 49 (7) (2008) 1107–1113.

[27] J. Jiao, F. Kang, J. Zhang, Z. Quan, W. Wen, X. Zhao, et al., Establishment and prospective validation of an SUVmax cutoff value to discriminate clinically signifi cant prostate cancer from benign prostate diseases in patients with suspected prostate cancer by 68G a-PSMA PET/CT: a real-world study, Theranostics 11 (17) (2021) 8396–8411.

[28] K. Yang, Y. Zhao, Y. Du, R. Tang, Evaluation of hippo pathway and CD133 in radiation resistance in small-cell lung cancer, JAMA Oncol. 2021 (2021) 8842554.

[29] W.H. Hsu, X. Zhao, J. Zhu, I.K. Kim, G. Rao, J. McCutcheon, et al., Checkpoint kinase 1 inhibition enhances cisplatin cytotoxicity and overcomes cisplatin resistance in SCLC by promoting mitotic cell death, J. Thorac. Oncol. 14 (6) (2019) 1032–1045.

[30] H. Zou, S.M. Thomas, Z.W. Yan, J.R. Grandis, A. Vogt, L.Y. Li, Human rhomboid family-1 gene RHBDF1 participates in GPCR-mediated transactivation of EGFR growth signals in head and neck squamous cancer cells, Faseb. J. 23 (2) (2009) 425–432.

[31] S.H. Barghout, P.S. Patel, X. Wang, G.W. Xu, S. Kavanagh, O. Halgas, et al., Preclinical evaluation of the selective small-molecule UBA1 inhibitor, TAK-243, in acute myeloid leukemia, Leukemia 33 (1) (2019) 37–51.

[32] G.R. Devi, P. Finetti, M.A. Morse, S. Lee, A. de Nonneville, S. Van Laere, et al., Expression of X-linked inhibitor of apoptosis protein (XIAP) in breast cancer is associated with shorter survival and resistance to chemotherapy, Cancers 13 (11) (2021).

[33] X. Ni, W. Kou, J. Gu, P. Wei, X. Wu, H. Peng, et al., TRAF6 directs FOXP3 localization and facilitates regulatory T-cell function through K63-linked ubiquitination, EMBO J. 38 (9) (2019).

[34] L. Wischhof, A. Gioran, D. Sonntag-Bensch, A. Piazzesi, M. Stork, P. Nicotera, et al., A disease-associated Aifm1 variant induces severe myopathy in knockin mice, Mol. Metabol. 13 (2018) 10–23.

[35] D.W. Wu, Y.C. Wang, L. Wang, C.Y. Chen, H. Lee, A low microRNA-630 expression confers resistance to tyrosine kinase inhibitors in EGFR-mutated lung adenocarcinomas via miR-630/YAP1/ERK feedback loop, Theranostics 8 (5) (2018) 1256–1269.

[36] C. Zhang, Z. Liu, X. Wang, B. Zhang, L. Cui, Q. Hu, et al., Cathepsin K promotes the proliferation of hepatocellular carcinoma cells through induction of SIAH1 ubiquitination and degradation, iScience 26 (6) (2023) 106852.

[37] J. Salimian, B. Baradaran, S. Azimzadeh Jamalkandi, A. Moridikia, A. Ahmadi, MiR-486-5p enhances cisplatin sensitivity of human muscle-invasive bladder cancer cells by induction of apoptosis and down-regulation of metastatic genes, Urologic oncology-seminars and original investigations 38 (9) (2020), 738.e739-738.e721.

[38] W. Sun, Y. Ma, P. Chen, D. Wang, MicroRNA-10a silencing reverses cisplatin resistance in the A549/cisplatin human lung cancer cell line via the transforming growth factor-β/Smad2/STAT3/STAT5 pathway, Mol. Med. Rep. 11 (5) (2015) 3854–3859.

[39] P. González-Alonso, S. Zazo, E. Martín-Aparicio, M. Luque, C. Chamizo, M. Sanz-Álvarez, et al., The hippo pathway transducers YAP1/TEAD induce acquired resistance to trastuzumab in HER2-positive breast cancer, Cancers 12 (5) (2020) null.

[40] S. Song, S. Honjo, J. Jin, S.S. Chang, A.W. Scott, Q. Chen, et al., The hippo coactivator YAP1 mediates EGFR overexpression and confers chemoresistance in esophageal cancer, Clin. Cancer Res. 21 (11) (2015) 2580–2590.

[41] K.W. Lee, S.S. Lee, S.B. Kim, B.H. Sohn, H.S. Lee, H.J. Jang, et al., Significant association of oncogene YAP1 with poor prognosis and cetuximab resistance in colorectal cancer patients, Clin. Cancer Res. 21 (2) (2015) 357–364.

[42] J. Yin, L. Wang, Y. Wang, H. Shen, X. Wang, L. Wu, Curcumin reverses oxaliplatin resistance in human colorectal cancer via regulation of TGF-β/Smad2/3 signaling pathway, OncoTargets Ther. 12 (2019) 3893–3903.

[43] S. Liang, Y. Liu, J. He, T. Gao, L. Li, S. He, Family with sequence similarity 46 member a confers chemo-resistance to ovarian carcinoma via TGF-β/Smad2 signaling, Bioengineered 13 (4) (2022) 10629–10639.

[44] P. Zhao, Y.G. Ma, Y. Zhao, D. Liu, Z.J. Dai, C.Y. Yan, et al., MicroRNA-552 deficiency mediates 5-fluorouracil resistance by targeting SMAD2 signaling in DNA-mismatch-repair-deficient colorectal cancer, Cancer chemoth pharm 84 (2) (2019) 427–439.

[45] S.K. Wu, B.J. Wang, Y. Yang, Y.J. Tian, J.J. Bao, X.H. Feng, et al., [Expressions of phosphorylated-Smad2 and PTEN in hepatocellular carcinomas and adjacent liver tissues], Zhonghua gan zang bing za zhi = Zhonghua ganzangbing bingzhi = Chinese journal of hepatology 15 (8) (2007) 567–571.

[46] K. Matsuzaki, C. Kitano, M. Murata, G. Sekimoto, K. Yoshida, Y. Uemura, et al., Smad2 and Smad3 phosphorylated at both linker and COOH-terminal regions transmit malignant TGF-beta signal in later stages of human colorectal cancer, Cancer Res. 69 (13) (2009) 5321–5330.

[47] F. Liu, W. Xie, Z. Liu, T. Roy, E. Bae, L. Wakefield, et al., Abstract 4940: role of Smad3 linker phosphorylation in breast cancer progression, Cancer Res. 75 (15_Supple) (2015), 4940-4940.

[48] S. Kaowinn, N. Yawut, S.S. Koh, Y.H. Chung, Cancer upregulated gene (CUG)2 elevates YAP1 expression, leading to enhancement of epithelial-mesenchymal transition in human lung cancer cells, Biochem bioph res co 511 (1) (2019) 122–128.

[49] Z. Yan, H. Zou, F. Tian, J.R. Grandis, A.J. Mixson, P.Y. Lu, et al., Human rhomboid family-1 gene silencing causes apoptosis or autophagy to epithelial cancer cells and inhibits xenograft tumor growth, Mol cancer ther 7 (6) (2008) 1355–1364.

[50] X. Wang, Y. Guo, L. Liu, J. Wei, J. Zhang, T. Xie, et al., YAP1 protein expression has variant prognostic significance in small cell lung cancer (SCLC) stratified by histological subtypes, Lung Cancer 160 (2021) 166–174.